Available online at www.sciencedirect.com

SciVerse ScienceDirect

Journal of the European Ceramic Society 32 (2012) 665–670

www.elsevier.com/locate/jeurceramsoc

Crystal structure and *ab initio* calculations of $CaZrO_3$

P. Stoch *, J. Szczerba, J. Lis, D. Madej, Z. Pędzich

AGH – University of Science and Technology, Faculty of Material Science and Ceramics, al. Mickiewicza 30, 30-059 Kraków, Poland

Received 20 January 2011; received in revised form 28 September 2011; accepted 1 October 2011
Available online 21 October 2011

Abstract

Calcium zirconate ($CaZrO_3$), because of its high melting point, low thermal expansion coefficient, high strength and excellent corrosion resistance against alkali oxides, is a good candidate for a novel refractory material. $CaZrO_3$ is mostly synthesized by the reaction in the solid state but the material obtained in such a way often suffers low bulk density, high porosity and other defects which lower its potential application value. To overcome these obstacles a novel synthesis method by an electric arc melting technique was proposed. The crystal structure of melted $CaZrO_3$ was compared with a conventionally synthesized material. According to X-ray measurements the obtained material has an orthorhombic perovskite-like structure. Its stoichiometry was confirmed by the scanning electron microscope and EDS analysis. The material is almost poreless with its density close to theoretical. The estimated crystal structure parameters were used to calculate the electronic structure of $CaZrO_3$ using the full potential linear augmented plane wave (FLAPW) method. It has been found that $CaZrO_3$ is an insulator with the energy band gap of 4.1 eV. The Ca–O bond is typically ionic while Zr–O bond is of a significant covalent character.

Keywords: $CaZrO_3$; Refractory; Arc melting; *Ab initio*; Electronic structure; Crystal structure; Perovskite

1. Introduction

Calcium zirconate is the only compound in the $CaO–ZrO_2$ system with the melting point of 2345 °C.[1] $CaZrO_3$ exists in two polymorphic forms. At a low temperature the orthorhombic form is stable up to about 1900 °C and the cubic form is stable at higher temperatures. The low temperature $CaZrO_3$ has the *Pbnm* perovskite-like structure with slightly deformed ZrO_6 octahedra. The high temperature calcium zirconate has the ideal cubic perovskite structure (*Pm3m*).[2,3]

$CaZrO_3$ is studied because of its unique physical properties. Doping by Al_2O_3, Y_2O_3, MgO or a small excess of CaO or ZrO_2 induce the oxygen ion conduction and this mechanism becomes predominant.[4–7] Because of its extremely high chemical durability it might be used as a sensor to measure oxygen activity in molten steel.[8] Due to its low loss tangent, high dielectric constant with the low temperature coefficient it can be used in multilayer ceramic capacitors and dielectric resonators, especially for microwave applications. Its high melting point, small thermal expansion coefficient, high strength and excellent corrosion resistance against alkali oxides and slags makes it a good candidate for a ceramic refractory material with wide applications.[9–12] $CaZrO_3$ relatively easily incorporates actinides into its crystal structure and because of its high chemical durability is considered as a host material for spent nuclear fuel immobilization.[13]

According to the $ZrO_2–CaO$ phase diagram as it was suggested in,[14] after calcination at 600 °C the $CaO–ZrO_2$ mixture forms such phases as the monoclinic solid solution ZrO_2, $CaZr_4O_9$, $CaZrO_3$ and CaO depending on CaO/ZrO_2 mole ratios. The compound $CaZr_4O_9$ (monoclinic symmetry) was found to be stable at $T < 1310\,°C \pm 40\,°C$ where it transforms to the cubic fluorite-type solid solution.[15] The eutectoid decomposition of the cubic solid solution occurs at $1140\,°C \pm 40\,°C$ with 17.0 ± 0.5 mol% CaO content.[15] Moreover, when the sample was sintered up to 2000 °C, two ordered phases, $CaZr_4O_9$ and $Ca_6Zr_{19}O_{44}$, were found out in the $ZrO_2–CaO$ system. Their upper limits of stability were determined to be $1235\,°C \pm 15\,°C$ and $1355\,°C \pm 15\,°C$ for $CaZr_4O_9$ and $Ca_6Zr_{19}O_{44}$, respectively. According to the $ZrO_2–CaO$ phase diagram, the liquid phase does not appear up until the temperature of $2250\,°C \pm 20\,°C$ and about 40 mol% CaO, which is significantly higher than 1700 °C applied in this experiment. On the other hand, according to Ref. 16, in the $CaZrO_3–CaO$

* Corresponding author.
E-mail address: p.stoch@cyf.gov.pl (P. Stoch).

0955-2219/$ – see front matter © 2011 Elsevier Ltd. All rights reserved.
doi:10.1016/j.jeurceramsoc.2011.10.011

subsystem the liquid phase does not appear up until the temperature of 2260 °C and about 70 mol% CaO.

The $CaZrO_3$ synthesis reaction proceeds in the solid state with the Ca^{2+} ions diffusion ZrO_2 structure as a dominating mass transfer mechanism. Its synthesis starts at about 900 °C and proceeds up to 1500 °C.[1] Calcium zirconate is the most often synthesized by the solid state reaction between CaO and ZrO_2 at 1300–1450 °C. The obtained powders are then formed and sintered in the temperature range 1700–1800 °C. The materials prepared by the above method have high porosity and lower bulk density,[1] suffer from the existence of CaO inclusions and other defects which lower their potential application value. Therefore other synthesis methods, such as wet chemical, amorphous precursor or mechanochemical methods are being studied.[17,18] In our studies we propose an electric arc melting technique to synthesize $CaZrO_3$. In this technique the melted material is placed in a well conducted crucible which is cooled by water and the crucible is one of electrodes. The second electrode is placed above the melted material. High electric current, which is flowing from the crucible via the melted material and protective gas atmosphere to the second electrode, causes a formation of an electric arc between the material and the second electrode. The electric arc temperature can exceed over 3000 °C and starts melting materials placed in the crucible. To obtain stable electric arc parameters the melted material should be well conducted. Therefore this technique was limited to melting conducting materials such as metals and their alloys.

The aim of our studies was to test the possibility of making refractory materials, especially using electric arc melting technique $CaZrO_3$ phase. Then their crystal structure had to be checked and the obtained results had to be compared with the material made by the standard solid state reaction synthesis. Finally, the measured crystal structure parameters were used to calculate the electronic band structure of $CaZrO_3$, prepared by both methods, to test how small changes in the crystal structure could affect it.

2. Experimental

Two different methods were used to synthesize $CaZrO_3$, i.e. melting in the electric arc and the standard solid state reaction method.

In both cases pure chemical $CaCO_3$ and ZrO_2 were mixed together in the proportion of the CaO to ZrO_2 ratio corresponding to $CaZrO_3$ stoichiometry. The specification of the starting materials is shown in Table 1. The obtained mixtures were homogenized by mechanical mixing using the vibratory zirconium ball mill and then pellets of 10 mm in diameter were pressed at 30 MPa.

Table 1
Specification of the starting materials.

Specification	Reagent	
	$CaCO_3$ (Chempur)	ZrO_2 (Merck)
Pure [%]	98.81	98.08
Median particle size [μm]	2.303	20.762
Specific surface area [m^2/g]	3.09	0.306

In the first method the pellets were melted in an arc furnace in the high purity argon atmosphere with contactless ignition. The electric current was slowly increased until the pellets started to melt. In this temperature the sample was kept for about 30 s and then the electric current was slowly decreased. To obtain better homogeneity of the sample it was turned over and the above procedure was repeated (sample A). During the arc melting of the materials the temperature of the melt can be locally very high, exceeding sometimes 3000 °C which can cause better mixing of the components but, on the other hand, it causes rapid evaporation of volatile elements. In the case of melting of oxides, due to their insulating character, the ignition of the electric arc could be very difficult and the size of a sample is limited to a few grams sample. The great advantage of the method consists in its simplicity (it does not need any special preparation of the starting materials, such as using high pressure pressing, etc., because the starting compounds are totally melted during the synthesis).

The reaction of the $CaZrO_3$ synthesis in the second method was carried out by the two step firing procedure. During the first step the pellets were heated up to 1700 °C and were held at this temperature for 10 h and then cooled down with the furnace. After this stage, the samples were ground to the grain size lower than 0.063 mm and again pressed under 30 MPa. Consequently, the samples were fired at 1700 °C with 10 h soaking time and cooled with the furnace (sample B). The linear shrinkage of the sample after the second firing was 3.48%.

The X-ray diffraction experiment was performed at room temperature using the powder diffraction method on Panalytical X'Pert-Pro diffractometer. The obtained diffraction patterns were analyzed using the Rietveld method,[19] implemented in the Fullprof code.[20]

Scanning electron microscopy (SEM) has been carried out on an electron microscope system (NovaNanoSem 200) with the energy dispersive spectrometer (EDS).

The electronic band structures of $CaZrO_3$ were calculated by the *ab initio* self-consistent full-potential linearized augmented plane waves (FLAPW) method as implemented in the WIEN2K code.[21] The generalized gradient approximation (GGA) in the parameterization of Perdew–Burke–Ernzerhof[22] was employed. The Brillouin zone integration was performed using a k mesh of 280k points in the irreducible Brillouin zone wedge. The muffin-tin radii were 2.2, 2.0 and 1.8 a.u. for Ca, Zr and O atoms, respectively. To control the size of the basis set for the wave functions, $R_{MT}K_{MAX}$ was set to 8.0, and the well-converged basis sets consist of about 1872 LAPW functions. The crystal structure parameters and atom positions were set according to the above XRD measurements.

3. Results and discussion

The measured diffraction patterns of samples A and B are presented in Figs. 1 and 2, respectively. In both cases there is no evidence of existence of secondary phases on the measured XRD patterns. The investigated $CaZrO_3$ crystallizes in the orthorhombic crystal structure *Pbmn* space group in which

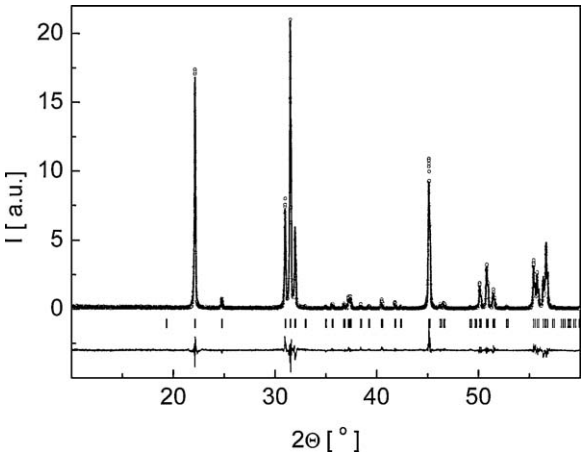

Fig. 1. The XRD pattern of the melted $CaZrO_3$ (sample A).

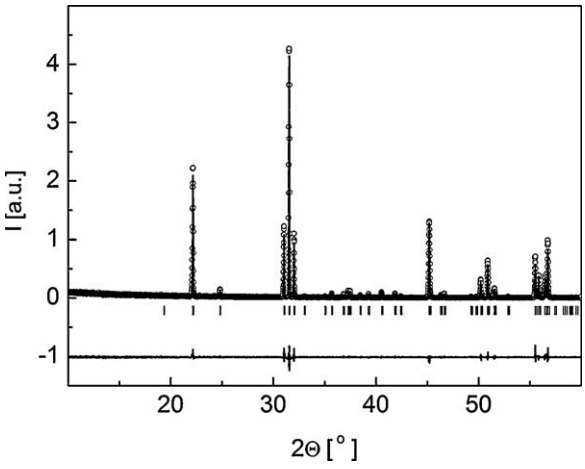

Fig. 2. The XRD pattern of the sintered $CaZrO_3$ (sample B).

the atoms occupy Wycoff's positions: Ca (4c) (x, 1/4, z), Zr (4b) (1/2, 0, 0), O (4c) (x, 1/4, z) and O (8d) (x, y, z). The obtained lattice parameters are summarized in Table 2.

As it can be clearly seen, the crystal structure parameters and atomic coordinates are in good agreement with the literature data.[3] The $CaZrO_3$ structure is composed of almost regular

Table 2
Crystal structure parameters of samples A and B.

	Sample A	Sample B	Literature[3]
a [Å]	5.5974(3)	5.5890(1)	5.5912(1)
b [Å]	8.0271(1)	8.0140(3)	8.0171(1)
c [Å]	5.7691(4)	5.7586(2)	5.7616(2)
Ca 4(c)			
x	0.0108	0.0114	0.0121
z	0.0478	0.0520	0.0496
O 4(c)			
x	0.5806	0.6090	0.6032
z	−0.0223	−0.0399	−0.0381
O 8(d)			
x	0.3002	0.3116	0.3026
y	0.0459	0.0504	0.0548
z	0.3069	0.3048	0.3007

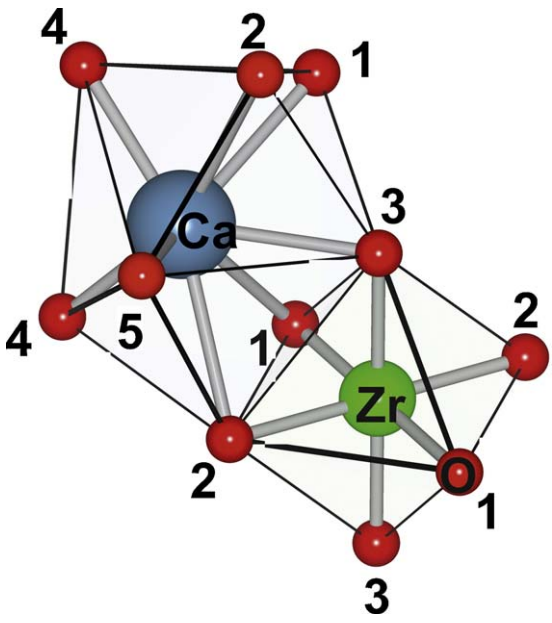

Fig. 3. Coordination spheres for Ca and Zr in $CaZrO_3$.

ZrO_6 octahedra which are rotated in relation to their positions in an ideal perovskite structure. Because of this rotation, the coordination of the Ca^{2+} ions is reduced from 12 in ideal perovskite to 8 in $CaZrO_3$.

Coordination spheres for Ca and Zr in $CaZrO_3$ are presented in Fig. 3. In Table 3 Zr–O distances are shown inside the ZrO_6 octahedra and inside the Ca coordination sphere, Zr–O, Ca–O angles are presented in Table 4. The evaluated mean Ca-O distances were 2.602 Å and 2.678 Å for sample A and B, respectively, and Zr–O 2.079 Å and 2.038 Å, respectively.

The scanning electron microscopy (SEM) micrograph of the arc melted sample is shown in Fig. 4a. As it can be seen from Fig. 4a, the microstructure of the arc melted $CaZrO_3$ is dense, poreless with the regular shape different size crystals. Their size varies from several to several tens of microns. In Fig. 5a, the microstructure of the sintered sample (sample B) is shown and its obtained density is about 90% of theoretical value (4.95 g/cm^3).[1] As it can be seen while comparing Figs. 4a and 5a in the melted material, there are almost no pores and the density of the melt should be very close to the theoretical one. Stoichiometries of the sample in both cases were confirmed by the EDS measurements (Figs. 4b and 5b).

Table 3
The Ca–O and Zr–O interatomic distances in coordination spheres for different O cations as described in Fig. 3.

	Sample A [Å]	Sample B [Å]
Zr–O(1)	2.049	2.031
Zr–O(2)	2.126	2.039
Zr–O(3)	2.061	2.044
Ca–O(1)	2.746	2.720
Ca–O(2)	2.781	2.752
Ca–O(3)	2.532	2.585
Ca–O(4)	2.395	2.635
Ca–O(5)	2.442	2.457

Table 4
The Ca–O and Zr–O interatomic distances in coordination spheres for different O cations as described in Fig. 3.

	Sample A [°]	Sample B [°]
O(2)–Zr–O(3)	89.91	88.04
O(3)–Zr–O(1)	91.69	90.81
O(2)–Zr–O(1)	89.44	89.02
O(1)–Ca–O(2)	69.94	62.85
O(1)–Ca–O(3)	65.55	66.27
O(1)–Ca–O(4)	117.61	118.13
O(1)–Ca–O(5)	132.21	129.05
O(2)–Ca–O(3)	67.61	64.14
O(2)–Ca–O(4)	161.17	165.64
O(2)–Ca–O(5)	68.40	66.36
O(3)–Ca–O(4)	131.12	130.08
O(3)–Ca–O(5)	87.88	88.60
O(4)–Ca–O(5)	109.85	112.00

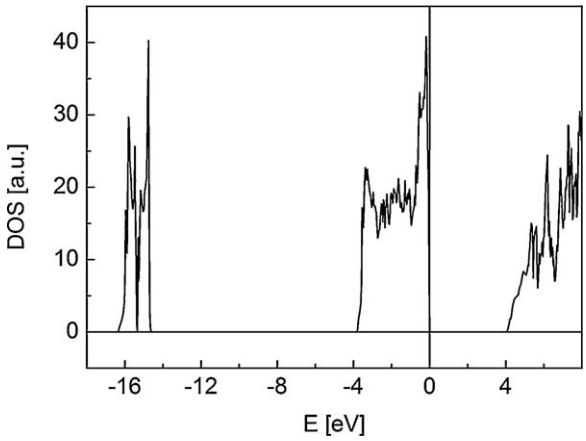

Fig. 6. Total density of states (DOS) of $CaZrO_3$.

The calculated total density of states (DOS) is presented in Fig. 6. The valence band is split into two regions. The lower one, which is quite a narrow band, starts at −16 eV and ends at about 14.5 eV. The upper band, wider than the lower one, ranges from about −4 eV to 0 eV. The end of the valence band is separated from a conduction band by a 4.1 eV energy band gap.

The calculated electronic band structure of the orthorhombic $CaZrO_3$ phase is shown in Fig. 7. Orthorhombic $CaZrO_3$ has been found to have a direct band gap at Γ-point ($k = (0,0,0)$) in the Brillouin zone. This wide gap indicates the presence of an insulating feature in the investigated material. The band gap of the $CaZrO_3$ is considered to be about 5.5 eV but this value has not been proved experimentally so far.[23]

The calculated partial density of states (PDOS) of $CaZrO_3$ is shown in Fig. 8. The lower region of the valence band comes mainly from O-2s states with a little contribution of the valence Zr-5p states and a negligible contribution of the Ca valence states. The upper region of the valence band is mainly composed of oxygen 2p states, Zr-4d states and a little contribution of Ca-3d states. Such a hybridization of the O-2p and Zr-4d states suggests a covalent character of the Zr–O bond whereas a negligible contribution of the Ca states to the valence band suggests an ionic character of the Ca–O bond. The conduction band starts at about 4 eV and is mainly composed of Ca-3d, hybridized with

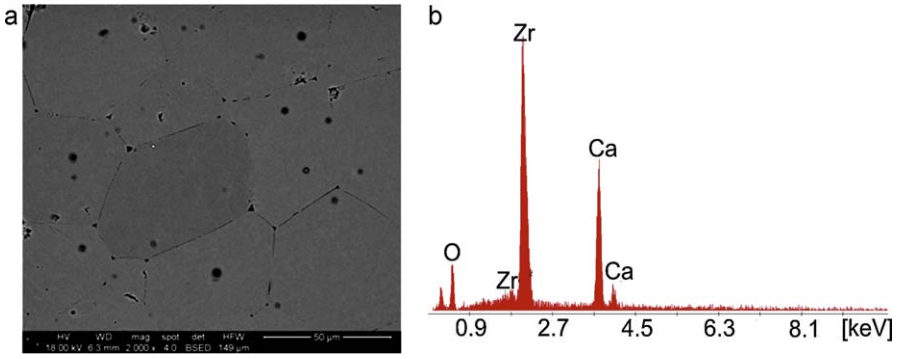

Fig. 4. (a) SEM micrograph and (b) EDS analysis of the arc melted $CaZrO_3$ (sample A).

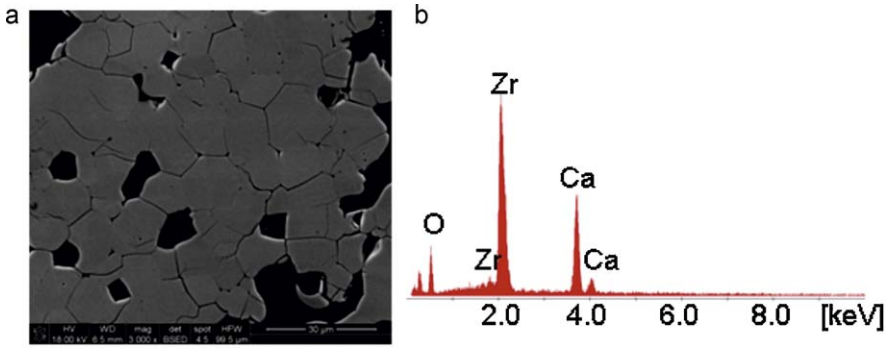

Fig. 5. (a) SEM micrograph and (b) EDS analysis of the sintered $CaZrO_3$ (sample B).

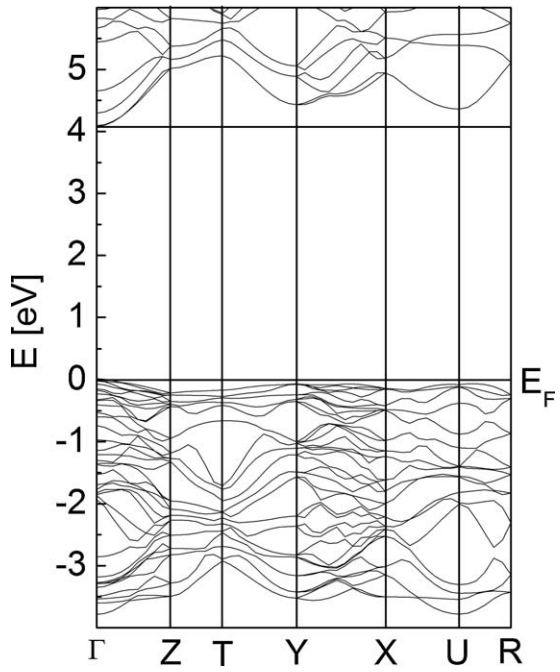

Fig. 7. Calculated electronic band structure of $CaZrO_3$.

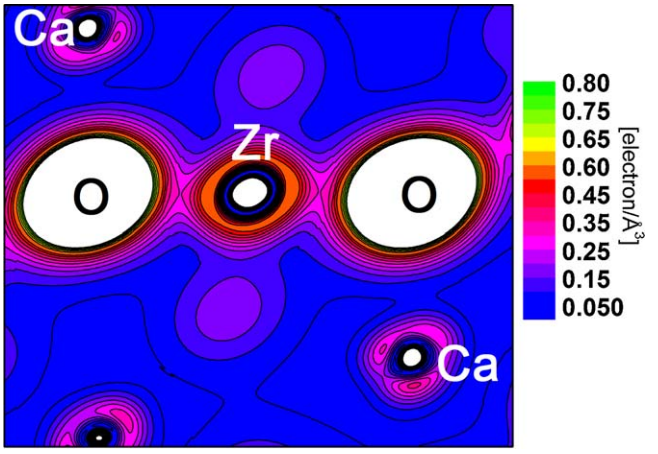

Fig. 9. Calculated valence charge distribution of $CaZrO_3$.

Table 5
Computed ion charges.

Ion	Sample A	Sample B
Ca	+1.571	+1.589
Zr	+2.560	+2.565
O(1)	−1.368	−1.341
O(2)	−1.387	−1.341
O(3)	−1.371	−1.373
O(4)	−1.363	−1.369
O(5)	−1.371	−1.374

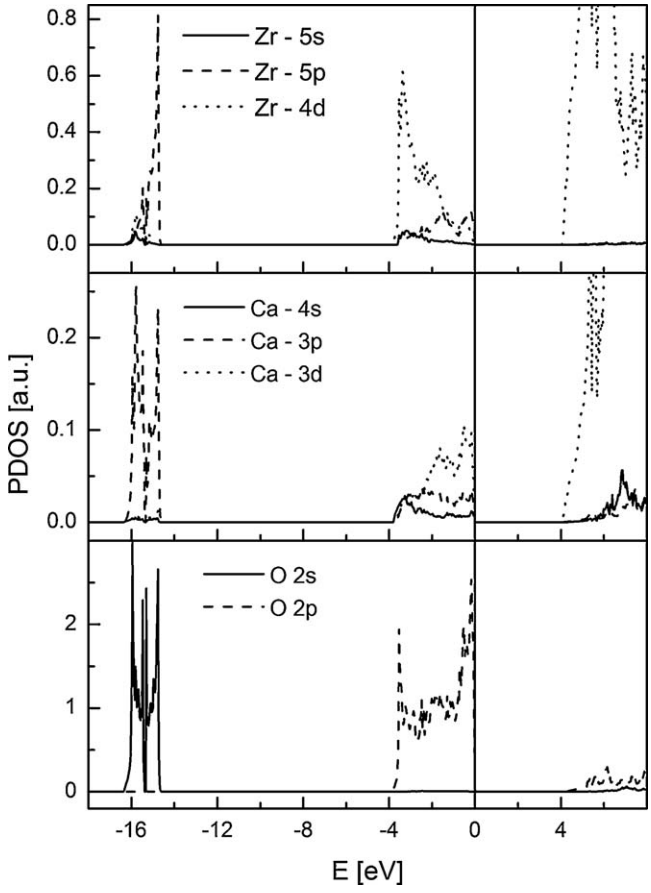

Fig. 8. Calculated partial density of states (PDOS) of $CaZrO_3$.

Zr-4d states. The obtained electronic band structure calculations are consistent and similar to the previously obtained in[3] for the high temperature cubic $CaZrO_3$ structure. In the case of the low temperature orthorhombic phase the band gap is a direct band gap of 4.1 eV whereas for the high temperature cubic structure the band gap becomes an indirect gap of 3.3 eV.[3] Such a behavior could indicate better insulating properties of the orthorhombic $CaZrO_3$ structure than the cubic one.

The charge distribution in $CaZrO_3$ is shown in Fig. 9. The valence charge density around Zr exhibits a slight directional distribution towards oxygen. The value of charge density in the middle between zirconium atoms and oxygen is about 0.35 electrons/Å^3. Such a behavior and hybridization between Zr-4d and O-2p observed at PDOS plots (Fig. 8), suggests a significant covalent Zr–O bond. On the other hand, the value of charge density between calcium and oxygen atoms is lower than 0.01 elctrons/Å^3, which proves the ionic character of the Ca–O bond. The estimated charges according to the Bader charge analysis are presented in Table 5.

The computed values of atomic charges were found to be +1.571 for Ca and +2.560 for Zr in the case of the arc melted sample (sample A) and in the case of sample B, +1.589 for Ca and +2.565 for Zr. The obtained values confirm mostly the ionic behavior of Ca and less Zr.

4. Conclusions

In our studies we proposed the arc melting technique to synthesize $CaZrO_3$. The detailed XRD studies confirmed the crystal

structure and stoichiometry of the investigated compound. When compared with the material obtained by the conventional solid state reaction method, the fused $CaZrO_3$ is poreless and has the density close to theoretical. There is no evidence of free CaO inclusions detected by the performed XRD and SEM + EDS analyses. The obtained results proved the usefulness of the arc melting technique in the synthesis of high purity $CaZrO_3$.

The first principle calculations were performed using the FLAWP method and the electronic band structure was obtained. Our calculation shows the existence of a strong covalent bonding between d states of zirconium and p-states of oxygen atoms. On the other hand, the Ca–O bond is almost of a pure ionic character. The wide band gap exhibits the insulating properties of the studied material. We did not observe any significant differences in the band structure of the material synthesized using the electric arc melting or the solids state synthesis method.

Acknowledgement

The work was partially supported by the grant no. N R15-0014-06 of the Polish Ministry of Science and Higher Education.

References

1. Szczerba J, Pędzich Z. The effect of natural dolomite admixtures on calcium zirconate–periclase materials microstructure evolution. *Ceram Int* 2010;**36**:535–47.
2. Koopmans HJA, van de Velde GMH, Gellings PJ. Powder neutron diffraction study of the perovskites $CaTiO_3$ and $CaZrO_3$. *Acta Crystallogr* 1983;**C39**:1323–5.
3. Hou ZF. Ab initio calculations of elastic modulus and electronic structures of cubic $CaZrO_3$. *Physica B* 2008;**403**:2624–8.
4. Manik SK, Pradhan SK. X-ray microstructure characterization of ball-milled nanocrystalline microwave dielectric $CaZrO_3$ by Rietveld method. *J Appl Crystallogr* 2005;**38**:291–8.
5. Wang CC, Akbar SA, Chen W, Schorr JR. High-temperature thermistors based on yttria and calcium zirconate. *Sens Actuators A* 1997;**58**:237–43.
6. Wang CC, Chen WH, Akbar SA, Alim MA. High-temperature a.c. electrical behaviour of polycrystalline calcium zirconate. *J Mater Sci* 1997;**32**:2305–12.
7. Wang CC, Xu X, Yu H. A study of the solid electrolyte Y_2O_3-doped $CaZrO_3$. *Solid State Ionics* 1998;**28/30**:542–5.
8. Janke D. Oxygen probes based on calcia-doped hafnia or calcium zirconate for use in metallic melts. *Metall Trans B* 1982;**13**:227–35.
9. Nadler MR, Fitzsimmoms ES. Preparation and properties of calcium zirconate. *J Am Ceram Soc* 1955;**38**:214–7.
10. Jonas S, Nadachowskis F, Szwagierczak D. A new non-silicate refractory of low thermal expansion. *Ceram Int* 1998;**24**:211–6.
11. Serena S, Sainz MA, Caballero A. A corrosion behavior of MgO/$CaZrO_3$ refractory matrix by clincker. *J Eur Ceram Soc* 2004;**24**:2399–406.
12. Róg G, Dudek M, Kozłowska-Róg A, Bućko M. Calcium zirconate: preparation, properties and application to the solid oxide galvanic cells. *Electrochim Acta* 2002;**47**:4523–9.
13. Smith KL, Colella M, Cooper R, Vance ER. Measured displacement energies of oxygen ions in titanates and zirconates. *J Nucl Mater* 2003;**321**:19–28.
14. Stubican VS, Ray SP. Phase equilibria and ordering in the system ZrO_2–CaO. *J Am Ceram Soc* 1977;**60**:534–7.
15. Hellmann JR, Stubican VS. Stable and metastable phase relations in the system ZrO_2–CaO. *J Am Ceram Soc* 1983;**66**:260–4.
16. Ruff O, Ebert F, Stephan E. Contributions to the ceramics of highly refractory material: II. System zirconia-lime. *Z Anorg Allg Chem* 1929;**180**:215–24.
17. Lee WJ, Wakahara A, Kim BH. Decreasing of $CaZrO_3$ sintering temperature with glass frit addition. *Ceram Int* 2005;**31**:521–4.
18. Dudek M. Oxide solid electrolytes as components of electro-chemical probes applied to measure activity of oxygen dissolved in liquid metals. *Ceramika* 2008;**103**:155–62.
19. Rietveld HM. A profile refinement method for nuclear and magnetic structures. *J Appl Crystallogr* 1969;**2**:65–71.
20. Rodriguez-Carvajal J. Recent advances in magnetic structure determination by neutron powder. *Diffr Phys B* 1993;**192**:55–69.
21. Blaha OP, Schwarz K, Madsen GKH, Kvasnicka D, Luitz J. *WIEN2k, an augmented plane wave + local orbitals program for calculating crystal properties*. Wien, Austria: Karlheinz Schwarz, Techn. Universität; 2001, ISBN 3-9501031-1-2.
22. Perdew JP, Burke K, Ernzerhof M. Generalized gradient approximation made simple. *Phys Rev Lett* 1996;**77**:3865–8.
23. Higuchi T, Yamaguchi S, Kobayashi K, Shind S, Tsukamoto T. Electronic structures in the bulk and surface states of protonic conductor $CaZrO_3$ by soft-X-ray spectroscopy. *Solid State Ionics* 2003;**162**(163):121–5.